LETTER

A New Approach for Personal Identification Based on dVCG

Jong Shill LEE†, Baek Hwan CHO†, Young Joon CHEE†, *Nonmembers*,
In Young KIM†*a), *Member, and* Sun I. KIM†, *Nonmember*

SUMMARY We propose a new approach to personal identification using derived vectorcardiogram (dVCG). The dVCG was calculated from recorded ECG using inverse Dower transform. Twenty-one features were extracted from the resulting dVCG. To analyze the effect of each feature and to improve efficiency while maintaining the performance, we performed feature selection using the Relief-F algorithm using these 21 features. Each set of the eight highest ranked features and all 21 features were used in SVM learning and in tests, respectively. The classification accuracy using the entire feature set was 99.53 %. However, using only the eight highest ranked features, the classification accuracy was 99.07 %, indicating only a 0.46 % decrease in accuracy compared with the accuracy achieved using the entire feature set. Using only the eight highest ranked features, the conventional ECG method resulted in a 93 % recognition rate, whereas our method achieved >99 % recognition rate, over 6 % higher than the conventional ECG method. Our experiments show that it is possible to perform a personal identification using only eight features extracted from the dVCG.

key words: *personal identification, ECG, dVCG, Dower transform, SVM*

1. Introduction

Human identification has potential applications in many different areas where the identity of a person needs to be determined, and to obtain even higher security levels, more complex system are required. Specific features of human beings need to be selected to recognize a person. Much work has been carried out on human face identification, voice recognition, palm recognition, and iris recognition. One of the problems with these identification methods is the fact that a specific biometric belonging to a certain person can still be used, even if the owner of the biometric is not present, or has even died. Therefore, many biometric hardware systems include a so-called liveness testing. In most cases, such liveness testing is difficult to measure [1], and a better and more efficient method to test the "liveness" of an applicant's biometric is needed.

The electrocardiogram (ECG) signal is an alternative inherent liveness biometric because of the significant fact that an ECG signal does not exist if the owner is not alive. Recently, efforts have been made to exploring the feasibility of using ECG as a new biometric measure for human identification. Biel et al. showed that automated human identification can be achieved by analyzing the 30 features monitored using a standard 12-lead reset ECG [2]. Shen et al. showed that human identity verification was feasible by applying template matching and a decision-based neural network to the seven features extracted from a single-lead ECG [3]. Kyoso et al. developed a human identification engine based on the four feature parameters of an ECG data sequence sampled on a beat-to-beat basis [4]. All of these researchers used time intervals (e.g., P wave duration, PQ interval, QRS interval, and QT interval) and amplitude in their studies. These temporal features (i.e., interval and amplitude) can vary depending on variables such as the time of day of the measurement or the physical condition of the subject. Noise and positioning of the electrode can also decrease the accuracy. In contrast, the spatial features of the cardiac electrical vector, represented by the vectorcardiogram (VCG) are not affected by the variables mentioned above. It is also expected that the vectorcardiographic loops will differ in shape and orientation from person to person. Therefore, it is possible to identify a person by features extracted from VCG.

In this work, we investigated a new approach for identifying humans using VCG. Firstly, we extracted 21 features from the derived vectorcardiogram (dVCG). Because it takes impractical time for personal identification to use all 21 features and there are some redundant features that do not contribute to the classification performance, we adopted the Relief-F algorithm to improve the computational efficiency and remove possible redundant features. Finally, we performed personal identification using a Support Vector Machine (SVM).

2. Materials and Methods

2.1 Data Acquisition

Ten healthy volunteers were enrolled in the study, and a standard 12-lead ECG data recording was made for each subject. Each recording was 10 s long, and was performed when the subject was at rest. Data acquisition was carried out at a sampling speed of 500 samples per second using a CardioTouch (Bionet Co., Korea). The recordings were performed approximately one hundred times for each subject over a three-month period.

Manuscript received September 10, 2007.
Manuscript revised December 19, 2007.
†The authors are with the Department of Biomedical Engineering, Hanyang University, Seoul, Korea.
*Corresponding author.
a) E-mail: iykim@hanyang.ac.kr
DOI: 10.1093/ietisy/e91–d.4.1201

2.2 Derived VCG

VCG have been widely investigated in the diagnosis of heart diseases, such as atrial fibrillation [5], premature ventricular contraction [6], and early ventricular repolarization [7]. The electrode positions of a Frank lead VCG are different from those of a 12-lead ECG, and must first be deduced by the recording technicians. Furthermore, using a Frank lead VCG in addition to a 12-lead ECG requires two recordings instead of one, and consequently increases the cost. Therefore, a method for calculating VCG from a conventional 12-lead ECG is more appealing [5], [8].

The derived VCG (dVCG) was calculated from each ECG using a method based on inverse Dower matrix [9]. Each of the orthogonal leads, X, Y, and Z, used to plot the VCG were linear combinations of the eight independent leads (I, II, and V1–V6) of a standard 12-lead ECG.

The dVCG in three-dimensional space, showing the frontal (XY) plane, the horizontal (XZ) plane, and the sagittal (YZ) plane of a subjects' standard 12-lead ECG is shown in Fig. 1. As shown in Fig. 1, the frontal plane provides useful information, such as shape and direction, and it is less complicated. Therefore, we used the dVCG in three-dimensional space and the frontal plane. In the frontal (XY) plane, the large vector loop (the QRS vector loop) represents the QRS complex and the small vector loop (the T vector loop) represents the T wave of the ECG. The QRS and T vector loops are denoted by the solid and dashed lines in the XY plane, respectively.

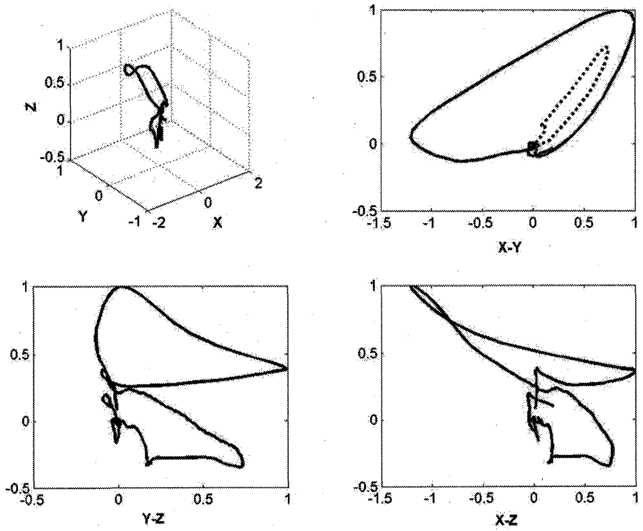

Fig. 1 The dVCG which was calculated using inverse Dower transform. In the XY plane, the solid and dashed lines denote the QRS and T vector loops, respectively.

2.3 Detection of the QRS Complex and T Wave

Detection of QRS complex and the T wave are required to calculate separate QRS and T vector loops. To detect the QRS complex, we used the QRS detection algorithm developed by Hamilton and Tompkins [10]. To detect the T wave, we used the QRS complex and the magnitude of the dVCG. The shape of the magnitude of the dVCG can be segmented into QRS and T wave regions. Therefore, we could easily

Table 1 The 21 features extracted from the dVCG.

	Feature	Description
1	VCG_{peak}	Maximum peak value in 3D space of the dVCG
2	$VCG_{azimuth}$	Azimuth angle of Feature 1
3	$VCG_{elevation}$	Elevation angle of Feature 1
4	QRS_{peak}	Maximum peak value in the QRS vector loop
5	QRS_{angle}	Angle of Feature 4
6	QRS_{area}	Area of the QRS vector loop
7	$QRS_{maxdist}$	Length of the major axis in the QRS vector loop
8	QRS_{maxang}	Angle of the major axis in the QRS vector loop
9	$QRS_{mindist}$	Length of the minor axis in the QRS vector loop
10	$QRS_{lwratio}$	Ratio of Feature 7 to Feature 9
11	T_{peak}	Maximum peak value in the T vector loop
12	T_{angle}	Angle of Feature 11
13	T_{area}	Area of the T vector loop
14	$T_{maxdist}$	Length of the major axis in the T vector loop
15	T_{maxang}	Angle of the major axis in the T vector loop
16	$T_{mindist}$	Length of the minor axis in the T vector loop
17	$T_{lwratio}$	Ratio of Feature 14 to Feature 16
18	$QRST_{diffang}$	QRS_{angle}–T_{angle}
19	$QRST_{diffarea}$	QRS_{area}–T_{area}
20	$QRST_{ratioarea}$	QRS_{area}/T_{area}
21	$QRST_{ratiopeak}$	QRS_{peak}/T_{peak}

separate the T wave interval by excluding the QRS region in the magnitude of the dVCG.

2.4 Feature Extraction

Data were acquired from each subject in 10 s periods, and usually contained 10 or more beats. Since the dVCG data taken from all those beats produced similar patterns, the average values were taken from each beat's dVCG trace. Twenty-one features were extracted from the dVCG data. Three features arose from the three-dimensional (3D) space, seven came from each QRS vector loop and T vector loop, and the others were the differential or proportional values obtained from the QRS and T vector loops. These 21 features are listed in Table 1.

2.5 Identification Using SVM and Relief-F Algorithm

We performed feature selection using the Relief-F algorithm [14] to reduce the dimensionality and to analyze the effect of each feature. We used a linear SVM with a pairwise coupling method as a classifier in our experiments [11]–[13], and compared the 10-fold cross validation accuracy by eliminating the lowest-ranked features one-by-one based on the Relief-F algorithm. We took advantage of the work of Weka [15] and LIBSVM [16] for the Relief-F method and SVM learning.

3. Results

To compare our proposed and a conventional ECG method, 14 features were extracted from the ECG, and these features were obtained from a conventional personal identification method utilizing the ECG. These features include: the PR interval (PR_{int}), the P amplitude (P_{amp}), the P-wave duration (P_{dur}), the Q amplitude (Q_{amp}), the Q-wave duration (Q_{dur}), the R amplitude (R_{amp}), the R-wave duration (R_{dur}), the S amplitude (S_{amp}), the S-wave duration (S_{dur}), the QRS duration (QRS_{dur}), the QRS amplitude (QRS_{amp}), the T amplitude (T_{amp}), the ST amplitude (ST_{amp}), and the QT interval (QT_{int}). These features are measured by the CardioTouch.

The Relief-F algorithm was applied to these 14 features and the results obtained are shown in Table 2. Note that the notation $w(f)$ is the output from the Relief-F algorithm, which means the relative importance of the features in terms of the ability for increasing the inter-class difference and the intra-class similarity. The foremost values were the P amplitude and QRS amplitude, along with the S amplitude and the S duration. We performed a classification using a linear SVM employing the pairwise coupling method in our experiments, and compared the 10-fold cross validation accuracy by eliminating the lowest-ranked features one-by-one. The results are denoted by the dashed line in Fig. 2. The recognition rate using the 14 features was 96.41 %, and the rate decreased as the number of features decreased. When we used eight features, the recognition rate was 93.31 %.

The 21 features extracted from the dVCG were ranked using the Relief-F algorithm, and are shown in Table 3. The highest values were the angle of the maximum peak value in the T vector loop and the angle of the major axis in the T vector loop. Next were the values of the length and the angle of the major axis in the QRS vector loop, followed by the length of the minor axis in the QRS vector loop and the size of the QRS vector loop. The difference between the size of the QRS and T vector loops came next. In the movement of the heart, the most dominant factor is the depolarization and repolarization of the ventricles. These were reflected in QRS and T waves. Because the repolarization takes longer time than depolarization, the morphology of T might influence more than QRS in classification.

The solid line in Fig. 2 shows that the recognition rates obtained using the specific 21 features extracted from the dVCG. These were processed using the same method used in the ECG personal identification. It shows that a recognition rate of 99.53 % was achieved using all 21 features and a recognition rate of 99.07 % was achieved using only the top eight ranked features. This suggests that by using only eight out of the 21 features, we can adequately produce an

Table 2 Rank of the 14 features extracted from the ECG.

Rank	$w(f)$	Feature
1	0.24614	R_{amp}
2	0.23788	QRS_{amp}
3	0.19385	S_{amp}
4	0.17273	S_{dur}
5	0.17217	QRS_{dur}
6	0.15941	Q_{dur}
7	0.15339	T_{amp}
8	0.11141	Q_{amp}
9	0.06685	R_{dur}
10	0.05171	ST_{amp}
11	0.03490	P_{amp}
12	0.03019	QT_{int}
13	0.00666	PR_{int}
14	0.00314	P_{dur}

Table 3 Rank of the 21 features extracted from the dVCG.

Rank	$w(f)$	Feature
1	0.26028	T_{angle}
2	0.25459	T_{maxang}
3	0.24278	$QRS_{maxdist}$
4	0.17459	QRS_{maxang}
5	0.16736	$QRS_{mindist}$
6	0.16552	QRS_{area}
7	0.16499	$QRST_{diffarea}$
8	0.16268	VCG_{peak}
9	0.14688	QRS_{peak}
10	0.14518	$VCG_{elevation}$
11	0.11549	$QRS_{lwratio}$
12	0.11397	$QRST_{diffang}$
13	0.10033	T_{area}
14	0.09135	$T_{maxdist}$
15	0.08369	$VCG_{azimuth}$
16	0.07818	T_{peak}
17	0.06905	$T_{mindist}$
18	0.05022	QRS_{angle}
19	0.03320	$QRST_{ratiopeak}$
20	0.02709	$T_{lwratio}$
21	0.00263	$QRST_{ratioarea}$

acceptable recognition rate.

When only eight features were used, the ECG method resulted in a recognition rate of approximately 93 % , where our proposed method achieved a recognition rate of >99 %, which was over 6 % higher than that obtained using the ECG method.

To measure the computation time, we implemented algorithms of feature extraction using Microsoft Embedded Visual C++® on Windows CE® (Pocket PC) platform with Intel XScale® PXA270 Processor. We measured the execution time by eliminating the lowest-ranked features one-by-one. The results are denoted by the diamond symbol in Fig. 2. It takes time 7,384 ms to extract all 21 features, whereas 3,376 ms for the eight highest ranked features. The results show that the computation time taken to extract the eight highest ranked features is much less (47.5 %) than that is required by extracting all 21 features.

It takes 7,038 ms (95.3 % of total computation time) to extract the four features of $QRS_{\max dist}$(359 ms), $QRS_{\min dist}$(718 ms), $T_{\max dist}$ (2,119 ms), $T_{\min dist}$(3,842 ms) (Fig. 2). It is known that the normal adult has the QRS duration of 60 ∼ 100 ms and T duration is 100 ∼ 250 ms [17]. Therefore number of samples of T loop is 2 ∼ 2.5 times than that of QRS loop. To calculate the distance of major and minor axis from each loop, we have to find the maximum distance of each pair of points on the loop. So the computation time is proportional to the square of number of samples of each loop. To calculate $T_{\max dist}$ and $T_{\min dist}$, it takes about six times than the time to calculate $QRS_{\max dist}$, $QRS_{\min dist}$. The time for $T_{\max dist}$(2,119 ms) was about 6 times of the time for $QRS_{\max dist}$(359 ms). However, we already have the information for $T_{\max dist}$ during the calculation process of the 2nd ranked feature of $T_{\max ang}$, no additional time is needed. The computation time for $QRS_{\min dist}$, $T_{\min dist}$ has similar properties as above. It takes 718 ms and 3,842 ms for $QRS_{\min dist}$ and $T_{\min dist}$.

The results in Fig. 2 showed a stable performance until the number of features decreased to a specific point, and then it decreased rapidly. These results indicate that the Relief-F algorithm can rank the features chosen in this study approximately.

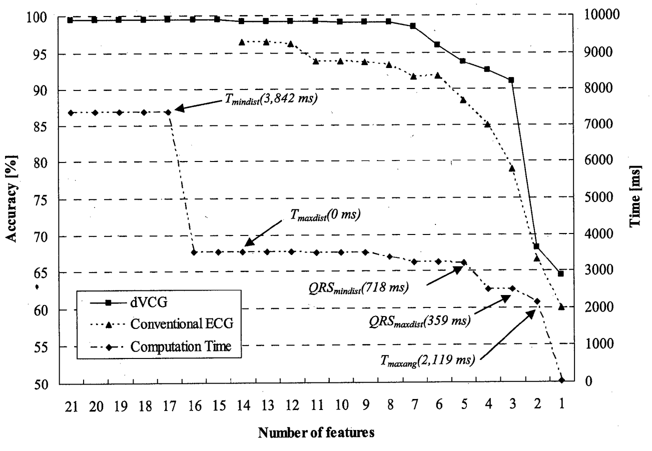

Fig. 2 Classification performance using the extracted features from a conventional ECG and the dVCG. And the computation time for the feature extraction from the dVCG.

4. Conclusions

We have studied a new approach for human identification using dVCG that can provide the spatial information of ECG. To identify a person by their spatial features extracted from a dVCG, we used a linear SVM as a classifier and calculated a 10-fold cross validation. The results show that by using only eight features, we can adequately produce an acceptable recognition rate and that a spatial ECG, such as a dVCG, can provide more defining features than those obtained using conventional temporal methods. Therefore, dVCG may be much more feasible in biometric recognition applications.

In this study, the standard 12 leads were used to acquire the dVCG, which will be somewhat troublesome to apply in the real world. However, the final results suggest that since the seven primary features were all taken from the XY plane, it may be possible to utilize only three leads instead of 12.

Further studies should include a reduction in the number of leads, and the stability of the dVCG with changes in the subject's various physical conditions, such as during exercise, drinking, and smoking. If these 21 features are stable under such various conditions, then dVCG could be a very feasible method to perform personal identification.

Acknowledgment

This study was supported by a Nano-bio technology development project, Ministry of Science & Technology, Republic of Korea. (2005-01249)

References

[1] D.W. John, N.M. Orlans, and P.T. Higgins, Biometrics—Identify assurance in the Information Age, pp.139–149, McGraw-Hill, USA, 2003.

[2] L. Biel, O. Pettersson, L. Philipson, and P. Wide, "ECG analysis: A new approach in human identification," IEEE Trans. Instrum. Meas., vol.50, no.3, pp.808–812, 2001.

[3] T.W. Shen, W.J. Tompkins, and Y.H. Hu, "One-lead ECG for identity verification," Proc. Second Joint EMBS/BMES Conference, pp.62–63, 2002.

[4] M. Kyoso and A. Uchiyama, "Development of an ECG identification system," Proc. 23rd Annual EMBS International Conference, pp.3721–3723, 2001.

[5] J. Carlson, R. Havmoller, A. Herreros, P. Platonov, R. Johansson, and B. Olsson, "Can orthogonal lead indicators of propensity to atrial fibrillation be accurately assessed from the 12-lead ECG?," Europace, vol.7, suppl. 2, pp.39–48, 2005.

[6] I. Christov, I. Jekova, and G. Bortolan, "Premature ventricular contraction classification by the Kth nearest-neighbours rule," Physiological Measurement, vol.26, no.2, pp.123–130, 2005.

[7] P. Dilaveris, A. Pantazis, E. Gialafos, J. Gialafos, P. Toutouzas, and C. Stefanadis, "Assessment of ventricular repolarization alterations in subjects with early repolarization," International Journal of Cardiology, vol.96, no.2, pp.273–279, 2004.

[8] L. Edenbrandt, A. Jakobsson, E. Lindvall, P.O. Bitzen, and O. Pahlm, "Increased prevalence of large bites in 12-lead vectorcardiograms of diabetic patients," Journal of Electrocardiology, vol.30, no.2, pp.91–96, 1997.
[9] L. Edenbrandt and O. Pahlm, "Vectorcardiogram synthesized from a 12-lead ECG: Superiority of the inverse Dower matrix," Journal of Electrocardiology, vol.21, no.4, pp.87–95, 1980.
[10] P.S. Hamilton and W.J. Tompkins, "Quantitative investigation of QRS detection rules using the MIT/BIH arrhythmia database," IEEE Trans. Biomed. Eng., vol.33, no.12, pp.1157–1165, 1986.
[11] V. Vapnik, The nature of statistical learning theory, Springer, New York, USA, 1995.
[12] C.J.C. Burges, "A tutorial on support vector machines for pattern recognition," Data Mining and Knowledge Discovery, vol.2, no.2, pp.121–167, 1998.
[13] T. Hastie and R. Tibshirani, "Classification by pairwise coupling," Annals of Statistics, vol.26, no.2, pp.451–471, 1998.
[14] I. Kononenko, "Estimating attributes: Analysis and extensions of relief," Proc. ECML'94, pp.171–182, Catania, Italy, April 1994.
[15] I.H. Witten and E. Frank, Data Mining: Practical machine learning tools and techniques, 2nd ed., Morgan Kaufman, San Francisco, USA, 2005.
[16] C.C. Chang and C.J. Lin, LIBSVM: A library for support vector machines, 2001. Software available at http://www.csie.ntu.edu.tw/~cjlin/libsvm
[17] R.J. Huszar, Basic Dysrhythmias : Interpretation & Management, 3rd ed., Mosby, 2001.